Geomechanics and Engineering, *Vol. 31, No. 1 (2022) 99-112*
https://doi.org/10.12989/gae.2022.31.1.099

The influence of Winkler-Pasternak elastic foundations on the natural frequencies of imperfect functionally graded sandwich beams

Mehmet Avcar*[1], Lazreg Hadji[2,3,4] and Recep Akan[1]

[1]*Department of Civil Engineering, Faculty of Engineering, Suleyman Demirel University, Cunur, Isparta, Türkiye*
[2]*Faculty of Civil Engineering, Ton Duc Thang University, Ho Chi Minh City 70000, Vietnam*
[3]*Department of Civil Engineering, University of Tiaret, BP 78 Zaaroura, Tiaret, 14000, Algeria*
[4]*Laboratory of Geomatics and Sustainable Development, University of Tiaret, 14000, Algeria*

(*Received May 7, 2022, Revised August 19, 2022, Accepted September 18, 2022*)

Abstract. The present study examines the natural frequencies (NFs) of perfect/imperfect functionally graded sandwich beams (P/IP-FGSBs), which are composed of a porous core constructed of functionally graded materials (FGMs) and a homogenous isotropic metal and ceramic face sheets resting on elastic foundations. To accomplish this, the material properties of the FGSBs are assumed to vary continuously along the thickness direction as a function of the volume fraction of constituents expressed by the modified rule of the mixture, which includes porosity volume fraction represented using four distinct types of porosity distribution models. Additionally, to characterize the reaction of the two-parameter elastic foundation to the Perfect/Imperfect (P/IP) FGSBs, the medium is assumed to be linear, homogeneous, and isotropic, and it is described using the Winkler-Pasternak model. Furthermore, the kinematic relationship of the P/IP-FGSBs resting on the Winkler-Pasternak elastic foundations (WPEFs) is described using trigonometric shear deformation theory (TrSDT), and the equations of motion are constructed using Hamilton's principle. A closed-form solution is developed for the free vibration analysis of P/IP-FGSBs resting on the WPEFs under four distinct boundary conditions (BCs). To validate the new formulation, extensive comparisons with existing data are made. A detailed investigation is carried out for the effects of the foundation coefficients, mode numbers (MNs), porosity volume fraction, power-law index, span to depth ratio, porosity distribution patterns (PDPs), skin core skin thickness ratios (SCSTR), and BCs on the values of the NFs of the P/IP-FGSBs.

Keywords: boundary conditions; FGMs; free vibration; porosity; sandwich beams; Winkler-Pasternak elastic foundations

1. Introduction

The mechanical features of soil have great importance on the dynamic responses of structures due to soil-structure interaction that examines how superstructure-foundation-soil interact with one another. For long years, the superstructure is designed without considering the soil-structure interaction, since, the most difficult aspect of this relationship is the behavior of the soil. However, recent studies have proved that the superstructure-foundation-soil interaction is an important factor in the design of structures, particularly that are subjected to dynamic responses such as natural frequency (NF). Therefore, it is critical to include the superstructure-foundation-soil interaction in modern structural design and analysis for the applications can be appropriately served (Bowles 1988, Dutta and Roy 2002, Rao 2010, Djedid *et al.* 2014, Das and Sivakugan 2018, Jia and Jia 2018, Kilicer *et al.* 2018, Bao and Liu 2020). In this context, the concept of beams resting on elastic foundations i.e. railway lines, highway asphalts, continuously supported pipes, and strip foundations is a critical instrument for simulation and analysis of structural, geotechnical, road, and railway engineering problems. Since soil has a very complex structure various approaches have been developed to model it. Among these approaches, the most adopted one is the Winkler elastic foundation model with a single parameter and assuming that the elastic foundation is composed of independent linear springs with continuous distribution (Winkler 1867). However, the displacement discontinuity between the loaded and unloaded parts of the foundation is an important challenge of this model, since the foundation surface does not show any discontinuities. For this reason, the Winkler-Pasternak elastic foundation (WPEF) model with two parameters, which is a physically more sensitive and mathematically simple model, has been developed (Pasternak 1954). In the WPEF model, the first parameter is the same as in the Winkler elastic foundation model, and the second one is the stiffness of the shear layer. (Hetényi 1946, Kerr 1964, Selvadurai 1979). The mechanical behaviors of structures resting on elastic foundations have been one of the most attractive topics of the open literature (Yokoyama 1996, Matsunaga 1999, Civalek and Acar 2007, Shen 2011, Calio and Greco 2013, Civalek 2013, Moniri Bidgoli *et al.* 2014, Kolahchi *et al.* 2015, El-Hassar *et al.* 2016, Saidi *et al.* 2016, Benahmed *et al.* 2017, Akgöz and Civalek 2018, Yahiaoui *et al.* 2018, Chaabane *et al.* 2019, Bouiadjra *et al.* 2020, Merzoug *et al.* 2020, Rabhi *et al.* 2020, Alnujaie *et al.* 2021, Alimoradzadeh and Akbas 2022, Asadi-Ghoozhdi *et al.*

*Corresponding author, Associate Professor
E-mail: mehmetavcar@sdu.edu.tr,
mehmetavcar@yahoo.com

ISSN: 2005-307X (Print), 2092-6219 (Online)

2022, Hebali *et al.* 2022, Liu *et al.* 2022, Tahir *et al.* 2022).

Composite materials, which have been used to construct structures with better qualities for centuries, are made by combining two or more elements with differing properties without dissolving or merging them. Thousands of years ago, ancient homes were constructed using composite materials in the form of mud bricks reinforced with straw. It is currently employed as a specialized material in instances where conventional materials are insufficient or whose qualities need to be increased, as engineers have several options for deciding the properties of the final composite throughout the production process. FGMs are a new kind of composite materials made of two components, ceramic, and metal, that exhibit progressive material property modification primarily in the thickness direction. In an FGM, the ceramic works as a heat-resistant material, while the metal offers structural rigidity. Due to their resistance to high temperatures, FGMs are used in a variety of industries, including aerospace, nuclear, and heat exchangers (Koizumi 1997, Kieback *et al.* 2003, Shen 2009, Naebe and Shirvanimoghaddam 2016, Rezaiee-Pajand and Masoodi 2016, Zouatnia *et al.* 2018, AlSaid-Alwan and Avcar 2020, Elmeichea *et al.* 2020, Bashiri *et al.* 2021, Bouafia *et al.* 2021, Madenci 2021, Pandey and Pradyumna 2021, Du *et al.* 2022). Sandwich composites are a form of composite material that consists of a thick but extremely light core material placed between two thin and hard upper and lower surface layers, and these structures have garnered considerable attention during the last few decades due to their desirable characteristics. Unlike laminated composites, adopting FG sandwich structures eliminates the issues of delamination, matrix cracking, stress concentrations at interfaces, and other damage processes. Scientists are particularly interested in the analysis of vibration of FGSBs with and without elastic foundations (Venkataraman and Sankar 2003, Ávila 2007, Amirani *et al.* 2009, Vo *et al.* 2014, Nguyen and Nguyen 2015, Nguyen *et al.* 2015, Vo *et al.* 2015, Vo *et al.* 2015, Mu and Zhao 2016, Nguyen *et al.* 2016, Tossapanon and Wattanasakulpong 2016, Trinh *et al.* 2016, Şimşek and Al-shujairi 2017, Kahya and Turan 2018, Rezaiee-Pajand *et al.* 2018, Rezaiee-Pajand *et al.* 2018, Songsuwan *et al.* 2018, Daikh *et al.* 2019, Sayyad and Ghugal 2019, Al-Furjan *et al.* 2021, Avcar *et al.* 2021, Kolahchi *et al.* 2021, Sayyad and Ghugal 2021, Van Vinh and Tounsi 2021, Zaitoun *et al.* 2021, Al-Furjan *et al.* 2022).

A family of materials characterized by high porosity, low density, and a large specific surface area, with foams serving as an example, is known as porous materials. By incorporating the concept of FGMs into porous materials, functionally graded porous materials (FGPMs) with continuous change in microstructure and porosity in a specified direction(s) are formed. It is possible to change their material properties to meet the needs of the structure they are going to be used. These advanced materials can be manufacturated through several different processes, such as powder sintering, freeze casting, gas foaming, selective laser melting, and more (Thieme *et al.* 2001, Hong *et al.* 2011, Zhou *et al.* 2011, He *et al.* 2014, Al-Saedi *et al.* 2018, Han *et al.* 2018, Wu *et al.* 2020). It is observed that structures made of FGPMs exhibit remarkable mechanical properties, such as high stiffness concerning a low specified weight, the efficient capacity of energy dissipation, and reduced thermal and electrical conductivity. Therefore, structures made of FGPMs are widely employed in lightweight constructions, aerospace, and the automotive sectors (Kitipornchai *et al.* 2017, Chen *et al.* 2019, Hamed *et al.* 2020, Rezaiee-Pajand and Masoodi 2022). Nowadays, the mechanical behaviors of structures composed of FGPMs with and without elastic foundations have become a hot topic for researchers (Wattanasakulpong and Ungbhakorn 2014, Al Rjoub and Hamad 2016, Galeban *et al.* 2016, Fouda *et al.* 2017, Akbaş 2018, Wattanasakulpong *et al.* 2018, Avcar 2019, Babaei *et al.* 2020, Rezaiee-Pajand *et al.* 2020, Al-Furjan *et al.* 2021, Al-Furjan *et al.* 2021, Farrokh and Taharpur 2021, Guellil *et al.* 2021, Hadji and Avcar 2021, Hadji and Avcar 2021, Madenci and Ozkilic 2021, Ramteke *et al.* 2021, Ramteke *et al.* 2021, Tahir *et al.* 2021, Xiao *et al.* 2021, Ramteke *et al.* 2022).

While many researchers have investigated the mechanical characteristics of FGSBs with and without elastic foundations, the number of studies on the vibration of FGSBs, including the effects of WPEFs and porosity at the same time, is still in the minority. Besides, the effect of the different BCs and PDPs interacting with beam and material characteristics have not been dealt with yet. This has resulted in the current research being concerned with the free vibration of P/IP-FGSBs resting on WPEFs under different BCs. To accomplish this, the material properties of the FGSBs are assumed to vary continuously along the thickness direction as a function of the volume fraction of constituents expressed by the modified rule of the mixture, which includes porosity volume fraction represented using four distinct types of porosity distribution models. Additionally, to characterize the reaction of the two-parameter elastic foundation to the P/IP FGSBs, the medium is assumed to be linear, homogeneous, and isotropic, and it is described using the Winkler-Pasternak model. Furthermore, the kinematic relationship of the P/IP-FGSBs resting on the Winkler-Pasternak elastic foundations is described using trigonometric shear deformation theory, and the motion equations are constructed using Hamilton's principle. A closed-form solution is developed for the free vibration analysis of P/IP-FGSBs resting on the WPEFs under four distinct BCs. To validate the new formulation, extensive comparisons with existing data are made. A detailed investigation is carried out forthe effects of the foundation coefficients, MNs, porosity volume fraction, power-law index, span to depth ratio, PDP, SCSTR, BCs on the values of the NFs of the P/IP-FGSBs.

The following sections comprise the paper. Section 2 contains definitions for the geometry and material characteristics of FGSBs. The governing equations for free vibration of P/IP-FGSBs are determined in Section 3 using Hamilton's principle and TrSDT. Section 4 establishes the analytical technique for solving the current problem under four distinct BCs. Section 5 contains numerical data and an analysis of the current situation. Section 6 is where conclusions are reached.

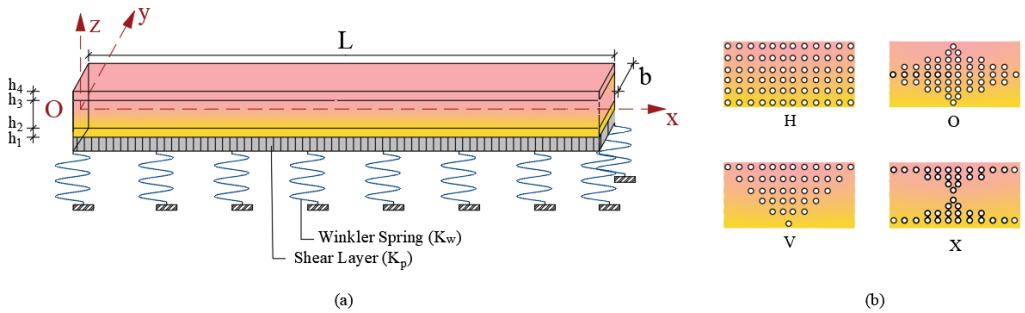

Fig. 1 (a) The geometry and (b) PDPs of the IP-FGSBs resting on WPEFs

Table 1 The layer schemes of FGSBs

Layer schemes	h_1	h_2	h_3	h_4
0-1-0	-h/2	-h/2	+h/2	+h/2
2-1-2	-h/2	-h/10	+h/10	+h/2
2-1-1	-h/2	0	+h/4	+h/2
1-1-1	-h/2	-h/6	+h/6	+h/2
2-2-1	-h/2	-h/10	+3h/10	+h/2
1-2-1	-h/2	-h/4	+h/4	+h/2
1-8-1	-h/2	-4h/10	+4h/10	+h/2

2. The geometry and material characteristics of FGSBs

Let us consider an IP-FGSB with a porous FG core and a homogeneous isotropic metal and ceramic face sheets resting on the WPEFs as shown in Fig. 1(a), where Fig. 1(b) illustrates porosity distributions of the FG core depending on four different porosity distribution patterns (PDPs), i.e., H-PDP, O-PDP, V-PDP, and X-PDP. The $x, y,$ and z axes are taken along the length, L, width b, and height, h of the FGSB, respectively.

From bottom to top, the FGSB is constructed of three elastic layers, particularly "Layer 1", "Layer 2", and "Layer 3". The bottom and top vertical locations, as well as the two interfaces between the layers, are designated by $h_1 = -h/2, h_2, h_3, h_4 = +h/2$ respectively. Because of the need for simplicity, the thickness of each layer from bottom to top, namely the skin-core-skin thickness ratio (SCSTR), is expressed by a combination of three integers, such as 1-8-1, 2-1-2, and so on. Table 1 shows the layer schemes of FGSBs versus SCSTR.

An assumption is made that the volume fraction of FGMs is governed by a power-law function in thickness directions as

$$V^{(1)}(z) = 0, z \in [h_1, h_2] \tag{1a}$$

$$V^{(2)}(z) = \left(\frac{z-h_2}{h_3-h_2}\right)^p, z \in [h_2, h_3] \tag{1b}$$

$$V^{(3)}(z) = 1, z \in [h_3, h_4] \tag{1c}$$

here, $V^{(n)}(z)$ stands for the volume fraction function of layer n, which may be expressed in terms of the volume fraction index p ($0 \le p \le \infty$) through the thickness of FGSBs.

For each layer, the effective features of the material of IP-FGSB are as follows:

For H-PDP

$$\begin{aligned} P^{(1)}(z) &= (P_c - P_m)V^{(1)}(z) + P_m \\ P^{(2)}(z) &= (P_c - P_m)V^{(2)}(z) + P_m - \frac{\alpha}{2}(P_c + P_m) \\ P^{(3)}(z) &= (P_c - P_m)V^{(3)}(z) + P_m \end{aligned} \tag{2}$$

For O-PDP

$$\begin{aligned} P^{(1)}(z) &= (P_c - P_m)V^{(1)}(z) + P_m \\ P^{(2)}(z) &= (P_c - P_m)V^{(2)}(z) + P_m - \frac{\alpha}{2}(P_c + \\ & P_m)\sqrt{\left(\frac{h_2-h_3}{2}\right)^2 - \left(z - \left(\frac{h_2+h_3}{2}\right)\right)^2} \\ P^{(3)}(z) &= (P_c - P_m)V^{(3)}(z) + P_m \end{aligned} \tag{3}$$

For V-PDP

$$\begin{aligned} P^{(1)}(z) &= (P_c - P_m)V^{(1)}(z) + P_m \\ P^{(2)}(z) &= (P_c - P_m)V^{(2)}(z) + P_m - \frac{\alpha}{2}(P_c + \\ & P_m)\left(\frac{z-h_2}{h_3-h_2}\right) \\ P^{(3)}(z) &= (P_c - P_m)V^{(3)}(z) + P_m \end{aligned} \tag{4}$$

For X-PDP

$$\begin{aligned} P^{(1)}(z) &= (P_c - P_m)V^{(1)}(z) + P_m \\ P^{(2)}(z) &= (P_c - P_m)V^{(2)}(z) + P_m - \frac{\alpha}{2}(P_c + \\ & P_m)\left|\frac{2z-(h_2+h_3)}{h_2-h_3}\right| \\ P^{(3)}(z) &= (P_c - P_m)V^{(3)}(z) + P_m \end{aligned} \tag{5}$$

where α ($\alpha \prec 1$) expresses the porosity volume fraction, and $P^{(i)} i = 1,2,3$ is the material properties, of the layers, respectively. Note that, while Young's modulus (E) and mass density (ρ) of the FG sandwich beam are supposed to vary constantly across the thickness, Poisson's ratio (ν) is assumed to be constant since its effect was found negligible (Delale and Erdogan 1983, Vo *et al.* 2015). Fig. 2 shows the variation of Young's modulus of the constituents for FGSBs with 1-8-1 SCSTR versus power-law index.

3. The governing equations of FGSBs

3.1 Basic assumptions

It is assumed that the middle surface of the FGSBs serves as the starting point for the Cartesian coordinate

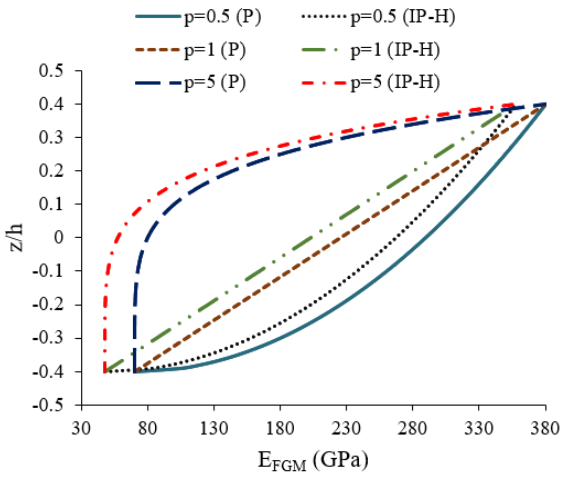

Fig. 2 The variation of volume fraction of the constituents for P/IP FGSBs with 1-8-1 SCSTR versus power-law index

system. Since the displacements are insignificant concerning the height of the FGSB, the stresses that are involved are supposed to be insignificant as well.

Bending w_b and w_s shear are two of the components that make up the transverse displacements. Only the x and t have any effect on these components.

$$w(x,z,t) = w_b(x,t) + w_s(x,t) \tag{6}$$

In comparison to in-plane stress, σ_x, the transverse normal stress, σ_z, is insignificant, and in the x-direction, the axial displacement is made up of extension, bending, and shear components as

$$u = u_0 + u_b + u_s \tag{7}$$

The displacements of the bending component, w_b, are thought to be the same as the displacements given by the classical beam theory. For this reason, the expression, u_b, can be written as

$$u_b = -z\frac{\partial w_b}{\partial x} \tag{8}$$

In combination with (w_s), the shear component (u_s) produces a hyperbolic variation in shear strain (γ_{xz}) and hence in shear stress (τ_{xz}) over the thickness of the beam, so that shear stress (τ_{xz}) is zero at the top and bottom faces of the FGSB. As a result, the expression for u_s may be written as

$$u_s = -f(z)\frac{\partial w_s}{\partial x} \tag{9}$$

where $f(z)$ is defined as a trigonometric function (Bekkaye *et al.* 2020)

$$f(z) = z - \frac{h}{\pi}\sin\left(\frac{\pi z}{h}\right) \tag{10}$$

3.2 Kinematics and constitutive equations

The displacement field of the trigonometric shear deformation theory (TrSDT) may be calculated using Eqs. (6)-(10) as a function of the assumptions stated in the previous section (Djedid *et al.* 2014)

$$u(x,z,t) = u_0(x,t) - z\frac{\partial w_b}{\partial x} - f(z)\frac{\partial w_s}{\partial x} \tag{11a}$$

$$w(x,z,t) = w_b(x,t) + w_s(x,t) \tag{11b}$$

The following strains are linked with the displacements in Eq. (11)

$$\varepsilon_x = \varepsilon_x^0 + z\,k_x^b + f(z)\,k_x^s \tag{12a}$$

$$\gamma_{xz} = g(z)\,\gamma_{xz}^s \tag{12b}$$

here

$$\varepsilon_x^0 = \frac{\partial u_0}{\partial x}, k_x^b = -\frac{\partial^2 w_b}{\partial x^2}, k_x^s = -\frac{\partial^2 w_s}{\partial x^2}, \gamma_{xz}^s = \frac{\partial w_s}{\partial x} \tag{12c}$$

$$g(z) = 1 - \frac{df(z)}{dz} \tag{12d}$$

Assuming the material used in the FGSBs follows Hooke's law, the stresses become

$$\sigma_x = Q_{11}(z)\,\varepsilon_x \text{ and } \tau_{xz} = Q_{55}(z)\,\gamma_{xz} \tag{13a}$$

where

$$Q_{11}(z) = E(z) \text{ and } Q_{55}(z) = \frac{E(z)}{2(1+\nu)} \tag{13b}$$

3.3 Equations of motion

Hamilton's principle is used to derive the equations of motion. The principle can be represented analytically (Rao 2019)

$$\int_{t_1}^{t_2}\left(\delta U + \delta U_{ef} - \delta K\right)dt = 0 \tag{14}$$

Here, δU is the virtual variation of the strain energy; δU_{ef} is the virtual variation of the elastic foundation's potential energy, and δK is the virtual variation of the kinetic energy. The strain energy change of the FGSB may be represented as

$$\begin{aligned}\delta\, U &= \int_0^L \int_{-\frac{h}{2}}^{\frac{h}{2}} (\sigma_x \delta\, \varepsilon_x + \tau_{xz}\delta\, \gamma_{xz})dzdx \\ &= \int_0^L \left(N_x \frac{d\delta\, u_0}{dx} - M_x^b \frac{d^2\delta\, w_b}{dx^2} - M_x^s \frac{d^2\delta\, w_s}{dx^2} \right. \\ &\qquad \left. + Q_{xz}\frac{d\delta\, w_s}{dx}\right) dx\end{aligned} \tag{15}$$

where N_x,M_x^b, M_x^s and Q_{xz} are the stress resultants and are defined as

$$\begin{aligned}(N_x, M_x^b, M_x^s) &= \int_{-\frac{h}{2}}^{\frac{h}{2}} (1, z, f(z))\sigma_x dz \\ \text{and } Q_{xz} &= \int_{-\frac{h}{2}}^{\frac{h}{2}} g(z)\tau_{xz} dz\end{aligned} \tag{16}$$

The change of the elastic foundation's potential energy as provided by

$$\begin{aligned}\delta U_{ef} = \int_0^L \Big[& K_W(w_b + w_s)\delta(w_b + w_s) - \\ & K_P \frac{\partial^2 (w_b + w_s)}{\partial x^2}\delta(w_b + w_s)\Big] dx\end{aligned} \tag{17}$$

where K_W and K_P are the stiffness coefficients of WPEFs, respectively.

The change in kinetic energy can be expressed in the following way

$$\begin{aligned}\delta K = \int_0^L \int_{-\frac{h}{2}}^{\frac{h}{2}} \rho(z)[\dot{u}\delta\dot{u} + \dot{w}\delta\dot{w}]\, dzdx = \\ \int_0^L \Big\{ I_0[\dot{u}_0\delta\dot{u}_0 + (\dot{w}_b + \dot{w}_s)(\delta\dot{w}_b + \delta\dot{w}_s)] - \\ I_1\left(\dot{u}_0\frac{d\delta\dot{w}_b}{dx} + \frac{d\dot{w}_b}{dx}\delta\dot{u}_0\right) + I_2\left(\frac{d\dot{w}_b}{dx}\frac{d\delta\dot{w}_b}{dx}\right) - \\ J_1\left(\dot{u}_0\frac{d\delta\dot{w}_s}{dx} + \frac{d\dot{w}_s}{dx}\delta\dot{u}_0\right) + K_2\left(\frac{d\dot{w}_s}{dx}\frac{d\delta\dot{w}_s}{dx}\right) \\ + J_2\left(\frac{d\dot{w}_b}{dx}\frac{d\delta\dot{w}_s}{dx} + \frac{d\dot{w}_s}{dx}\frac{d\delta\dot{w}_b}{dx}\right)\Big\} dx\end{aligned} \tag{18}$$

where dot-superscript convention implies the differentiation concerning the time variable t; $\rho(z)$ is the mass density; and $(I_0, I_1, J_1, I_2, J_2, K_2)$ are the mass inertias defined as

$$(I_0, I_1, J_1, I_2, J_2, K_2) = \int_{-\frac{h}{2}}^{\frac{h}{2}} (1, z, f, z^2, zf, f^2)\rho(z)dz \tag{19}$$

The related equations of motion are derived by substituting the expressions for δU, δU_{ef}, and δK from Eqs. (15), (17), and (18) into Eq. (14) and integrating the displacement gradients by parts and setting the coefficients of δu_0, δw_b and δw_s to zero separately

$$\delta u_0: \quad \frac{dN_x}{dx} = I_0\ddot{u}_0 - I_1\frac{d\ddot{w}_b}{dx} - J_1\frac{d\ddot{w}_s}{dx} \tag{20a}$$

$$\begin{aligned}\delta w_b: \quad \frac{d^2M_b}{dx^2} + K_P\left(\frac{d^2(w_b+w_s)}{dx^2}\right) - K_W(w_b + w_s) = \\ I_0(\ddot{w}_b + \ddot{w}_s) + I_1\frac{d\ddot{u}_0}{dx} - I_2\frac{d^2\ddot{w}_b}{dx^2} - J_2\frac{d^2\ddot{w}_s}{dx^2}\end{aligned} \tag{20b}$$

$$\begin{aligned}\delta w_s: \quad \frac{d^2M_s}{dx^2} + \frac{dQ_{xz}}{dx} + K_P\left(\frac{d^2(w_b+w_s)}{dx^2}\right) - K_W(w_b + \\ w_s) = I_0(\ddot{w}_b + \ddot{w}_s) + J_1\frac{d\ddot{u}_0}{dx} - J_2\frac{d^2\ddot{w}_b}{dx^2} - K_2\frac{d^2\ddot{w}_s}{dx^2}\end{aligned} \tag{20c}$$

By including Eq. (16) into Eq. (20), the equations of motion may be expressed in terms of displacements (u_0,w_b,w_s), and the associated equations take the form

$$A_{11}\frac{\partial^2 u_0}{\partial x^2} - B_{11}\frac{\partial^3 w_b}{\partial x^3} - B_{11}^s\frac{\partial^3 w_s}{\partial x^3} = I_0\ddot{u}_0 - I_1\frac{d\ddot{w}_b}{dx} - J_1\frac{d\ddot{w}_s}{dx} \tag{21a}$$

$$\begin{aligned}B_{11}\frac{\partial^3 u_0}{\partial x^3} - D_{11}\frac{\partial^4 w_b}{\partial x^4} - D_{11}^s\frac{\partial^4 w_s}{\partial x^4} + K_P\left(\frac{d^2(w_b+w_s)}{dx^2}\right) - \\ K_W(w_b + w_s) \\ = I_0(\ddot{w}_b + \ddot{w}_s) + I_1\frac{d\ddot{u}_0}{dx} - I_2\frac{d^2\ddot{w}_b}{dx^2} - J_2\frac{d^2\ddot{w}_s}{dx^2}\end{aligned} \tag{21b}$$

$$\begin{aligned}B_{11}^s\frac{\partial^3 u_0}{\partial x^3} - D_{11}^s\frac{\partial^4 w_b}{\partial x^4} - H_{11}^s\frac{\partial^4 w_s}{\partial x^4} + A_{55}^s\frac{\partial^2 w_s}{\partial x^2} + \\ K_P\left(\frac{d^2(w_b+w_s)}{dx^2}\right) - K_W(w_b + w_s) \\ = I_0(\ddot{w}_b + \ddot{w}_s) + J_1\frac{d\ddot{u}_0}{dx} - J_2\frac{d^2\ddot{w}_b}{dx^2} - K_2\frac{d^2\ddot{w}_s}{dx^2}\end{aligned} \tag{21c}$$

where A_{11}, D_{11}, etc., are the stiffnesses of FGSBs, and are defined by

$$\begin{aligned}\left(A_{ij}, A_{ij}^s, B_{ij}, D_{ij}, B_{ij}^s, D_{ij}^s, H_{ij}^s\right) \\ = \int_{-\frac{h}{2}}^{\frac{h}{2}} Q_{ij}(1, g^2(z), z, z^2, f(z), z\,f(z), f^2(z))dz\end{aligned} \tag{22}$$

4. Closed-form solution of FGSBs under different BCs

It is feasible to build a closed-form solution for FGSBs that applies to a variety of BCs. This is accomplished by taking into consideration the following BCs for the arbitrary ends of the FGSBs:

Simply supported (S) ends

$$w_b = w_s = 0 \text{ at } x = 0, L \tag{23}$$

Clamped (C) ends

$$u_0 = w_b = \frac{\partial w_b}{\partial x} = w_s = \frac{\partial w_s}{\partial x} = 0 \text{ at } x = 0, L \tag{24}$$

Free (F) ends

$$N_x = \frac{\partial M_x}{\partial x} = Q_x = M_x = 0 \text{ at } x = 0, L \tag{25}$$

The displacements that satisfy the BCs can be defined as follows

$$\begin{Bmatrix} u_0 \\ w_b \\ w_s \end{Bmatrix} = \begin{Bmatrix} U_m X_m' e^{i\omega t} \\ W_{bm} X_m e^{i\omega t} \\ W_{sm} X_m e^{i\omega t} \end{Bmatrix} \tag{26}$$

where ω is the eigenfrequency associated with the m_{th} eigenmode, and U_m, W_{bm} and W_{sm} are random parameters to be calculated. The admissible functions that satisfy at least the geometric BCs defined in Eqs. (23)-(25) and approximations of deflected FGSBs are as follows (Reddy 2003):

S-S BCs

$$X_m(x) = \sin(\beta_m x), \beta_m = m\frac{\pi}{L}, m = 1,2,\ldots \tag{27}$$

C-C BCs

$$\begin{aligned}X_m(x) = \sin(\beta_m x) - \sinh(\beta_m x) \\ - \psi_m[\cos(\beta_m x) - \cosh(\beta_m x)] \\ \psi_m = [\sin(\beta_m L) - \sinh(\beta_m L)] \\ /[\cos(\beta_m L) - \cosh(\beta_m L)] \\ \beta_m = \frac{(m + 0.5)}{L}\pi\end{aligned} \tag{28}$$

C-S BCs

$$\begin{aligned}X_m(x) = \sin(\beta_m x) - \sinh(\beta_m x) \\ - \psi_m[\cos(\beta_m x) - \cosh(\beta_m x)] \\ \psi_m = [\sin(\beta_m L) + \sinh(\beta_m L)] \\ /[\cos(\beta_m L) + \cosh(\beta_m L)] \\ \beta_m = \frac{(m + 0.25)}{L}\pi\end{aligned} \tag{29}$$

C-F BCs

$$\begin{aligned}X_m(x) = \sin(\beta_m x) - \sinh(\beta_m x) \\ - \psi_m[\cos(\beta_m x) - \cosh(\beta_m x)] \\ \psi_m = [\sin(\beta_m L) - \sinh(\beta_m L)] \\ /[\cos(\beta_m L) - \cosh(\beta_m L)] \\ \beta_1 = \frac{1.875}{L}, \beta_2 = \frac{4.694}{L}, \beta_3 = \frac{7.855}{L}, \beta_4 = \frac{10.966}{L}, \\ \beta_n = \frac{(m - 0.25)}{L}\pi \text{ for } n \geq 5\end{aligned} \tag{30}$$

The analytical solutions are obtained by substituting

Table 2 Comparison of the DNFs of P-FG beams resting on elastic foundations

Mode	k_w	k_p	Source	p					
				0	1	2	5	10	∞
1	0	0	Present	5.1531	3.9907	3.6263	3.3998	3.2811	2.6775
			Mechab *et al.* (2017)	5.1528	3.9904	3.6268	3.4028	3.2825	2.6773
			Sayyad and Ghugal (2018)	5.1453	3.9826	3.6184	3.3917	3.2727	2.6734
	0.1	0	Present	5.3118	4.2301	3.9046	3.7156	3.6186	3.0988
			Mechab *et al.* (2017)	5.3116	4.2299	3.9051	3.7183	3.6199	3.0987
			Sayyad and Ghugal (2018)	5.3038	4.2216	3.8961	3.7066	3.6094	3.0942
	0.1	0.1	Present	6.6786	6.1089	5.9934	5.9976	6.0056	5.7979
			Mechab *et al.* (2017)	6.6779	6.1073	5.9916	5.9964	6.0030	5.7904
			Sayyad and Ghugal (2018)	6.6689	6.0973	5.9810	5.9830	5.9909	5.7903
2	0	0	Present	17.8868	14.0138	12.6411	11.5324	11.0216	9.2938
			Mechab *et al.* (2017)	17.8780	14.0080	12.6420	11.5550	11.0290	9.2895
			Sayyad and Ghugal (2018)	17.5890	13.7540	12.3880	11.2600	10.7480	9.1392
	0.1	0	Present	17.9313	14.0804	12.7194	11.6253	11.1230	9.4187
			Mechab *et al.* (2017)	17.9230	14.0750	12.7210	11.6480	11.1310	9.4149
			Sayyad and Ghugal (2018)	17.6330	13.8200	12.4650	11.3510	10.8480	9.2623
	0.1	0.1	Present	19.6073	16.4948	16.4948	14.8290	14.5669	13.4450
			Mechab *et al.* (2017)	19.6030	16.4890	15.4910	14.8360	14.5590	13.4090
			Sayyad and Ghugal (2018)	19.2870	16.2000	15.2000	14.4930	14.2240	13.2400
3	0	0	Present	34.2344	27.1152	24.3237	21.6943	20.5581	17.7879
			Mechab *et al.* (2017)	34.1840	27.0810	24.3100	21.7400	20.5620	17.7620
			Sayyad and Ghugal (2018)	32.3240	25.5380	22.8120	20.1170	19.0030	16.7940
	0.1	0	Present	34.2572	27.1485	24.3632	21.7429	20.6120	17.8520
			Mechab *et al.* (2017)	34.2070	27.1150	24.3490	21.7880	20.6170	17.8270
			Sayyad and Ghugal (2018)	32.3460	25.5700	22.8490	20.1630	19.0530	16.8550
	0.1	0.1	Present	36.2208	29.9557	27.6329	25.6793	24.9218	22.8216
			Mechab *et al.* (2017)	36.1930	29.9360	27.6190	25.6990	24.9010	22.7360
			Sayyad and Ghugal (2018)	34.2230	28.2610	25.9800	23.8810	23.1070	21.6260

Eqs. (26) into Eqs. (21a)-(21d) (21c).

$$\left(\begin{bmatrix} a_{11} & a_{12} & a_{13} \\ a_{21} & a_{22} & a_{23} \\ a_{31} & a_{32} & a_{33} \end{bmatrix} - \omega^2 \begin{bmatrix} m_{11} & m_{12} & m_{13} \\ m_{21} & m_{22} & m_{23} \\ m_{31} & m_{32} & m_{33} \end{bmatrix}\right) \begin{Bmatrix} U_m \\ W_{bm} \\ W_{sm} \end{Bmatrix} = \begin{Bmatrix} 0 \\ 0 \\ 0 \end{Bmatrix} \tag{31}$$

where

$$\begin{gathered} a_{11} = \int_0^L A_{11}\, X_m^{''} X_m^{'} dx,\ a_{12} = \int_0^L -B_{11}\, X_m^{''} X_m^{'} dx, \\ a_{13} = \int_0^L -B_{11}^s\, X_m^{''} X_m^{'} dx, \\ a_{21} = \int_0^L B_{11}\, X_m^{''''} X_m dx,\ a_{22} = \int_0^L \left(-D_{11} X_m^{''''} + K_w X_m + K_p X_m^{''}\right) X_m dx, \\ a_{23} = \int_0^L \left(-D_{11}^s X_m^{''''} + K_w X_m + K_p X_m^{''}\right) X_m dx, \\ a_{31} = \int_0^L -B_{11}^s\, X_m^{''''} X_m dx, \\ a_{32} = \int_0^L \left(-D_{11}^s X_m^{''''} + K_w X_m + K_p X_m^{''}\right) X_m dx, \\ a_{33} = \int_0^L \left(-H_{11}^s X_m^{''''} + A_{55}^s X_m^{''} + K_w X_m + K_p X_m^{''}\right) X_m dx \end{gathered} \tag{32}$$

$$\begin{gathered} m_{11} = -I_0 \int_0^L X^{'} X^{'} dx\,, m_{12} = I_1 \int_0^L X^{'} X^{'} dx\,, m_{13} = J_1 \int_0^L X^{'} X^{'} dx \\ m_{21} = -I_1 \int_0^L X^{''} X dx\,, m_{22} = -\int_0^L \left(I_0 X - I_2 X^{''}\right) X dx\,, m_{23} = -\int_0^L \left(I_0 X + J_2 X^{''}\right) X dx \\ m_{31} = -J_1 \int_0^L X^{''} X dx\,, m_{32} = -\int_0^L \left(I_0 X - J_2 X^{''}\right) X dx\,, m_{33} = -\int_0^L \left(I_0 X - K_2 X^{''}\right) X dx \end{gathered} \tag{33}$$

5. Numerical results and discussions

This section focuses on the current problem using numerical examples. To begin, comparisons are done to demonstrate the existing formulations' validity. Then, the influences of elastic foundations, porosity, number of modes, changes in material properties, and geometrical features on the dimensionless natural frequencies (DNFs) of the P/IP-FGSBs are then investigated using parametrical investigations. Unless otherwise stated, the P/IP-FGSBs are supposed to be comprised of Al (metal) and Al_2O_3 (ceramic), and the material characteristics are taken to be $E_m = 70$ GPa, $\nu_m = 0.3$, $\rho_m = 2702\,\frac{\text{kg}}{\text{m}^3}$; $E_c = 380$ GPa, $\nu_c = 0.3$, $\rho_c = 3960$ kg/m^3. Furthermore, the following dimensionless parameters are applied

$$\Omega = \frac{\omega L^2}{h}\sqrt{\frac{\rho_m}{E_m}};\ k_w = \frac{K_w L^2}{E_m h};\ k_p = \frac{K_p}{E_m h} \tag{34}$$

where $\Omega, k_w,$ and k_p are DNF, dimensionless foundation coefficients of Winkler, and shear layers, respectively. Note that, $k_w = k_p = 0$, corresponds to the foundationless case, $\alpha = 0$ represents the perfect FGSB, 0-1-0 SCSTR indicates completely FG beams, in all examples.

5.1 Comparison studies

Study 1: Table 2 compares the DNFs of the first three

Table 3 Comparision of DFNFs of FGSBs without elastic foundations

SCSTR	Source	$L/h=5$						$L/h=20$					
		$p=0$	$p=0.5$	$p=1$	$p=2$	$p=5$	$p=10$	$p=0$	$p=0.5$	$p=1$	$p=2$	$p=5$	$p=10$
2-1-2	Present	3.6636	3.5849	3.5465	3.5122	3.4859	3.4781	3.8137	3.7411	3.7073	3.6791	3.6617	3.6590
	Kahya and Turan (2018)	3.6943	3.6178	3.5795	3.5431	3.5083	3.4907	3.8160	3.7437	3.7098	3.6815	3.6636	3.6602
2-1-1	Present	3.5226	3.4999	3.4896	3.4818	3.4779	3.4777	3.6806	3.6816	3.6878	3.7008	3.7226	3.7351
	Kahya and Turan (2018)	3.5374	3.5245	3.5203	3.5175	3.5111	3.5013	3.6818	3.6837	3.6903	3.7039	3.7254	3.7374
1-1-1	Present	3.8161	3.6627	3.5878	3.5239	3.4821	3.4734	3.9719	3.8229	3.7534	3.6994	3.6754	3.6784
	Kahya and Turan (2018)	3.8479	3.6964	3.6219	3.5564	3.5048	3.4831	3.9706	3.8220	3.7526	3.6986	3.6739	3.6760
2-2-1	Present	3.6636	3.5699	3.5288	3.4983	3.4819	3.4783	3.8137	3.7409	3.7176	3.7143	3.7377	3.7548
	Kahya and Turan (2018)	3.6891	3.6027	3.5674	3.5436	3.5273	3.5126	3.8157	3.7435	3.7207	3.7180	3.7417	3.7580
	Nguyen *et al.* (2016)	3.7142	3.6270	3.5885	3.5589	3.5411	3.5352	3.8647	3.7990	3.7784	3.7756	3.7966	3.8110
	Nguyen *et al.* (2015)	3.6624	3.5692	3.5292	3.5002	3.4858	3.4830	3.8136	3.7406	3.7177	3.7144	3.7380	3.7552
1-2-1	Present	4.0698	4.0698	3.6640	3.5526	3.4889	3.4791	4.2446	3.9701	3.8388	3.7401	3.7079	3.7210
	Kahya and Turan (2018)	4.1067	3.8362	3.7022	3.5913	3.5222	3.5007	4.2473	3.9732	3.8417	3.7433	3.7108	3.7231
	Nguyen *et al.* (2016)	4.0996	3.8438	3.7172	3.6119	3.5513	3.5413	4.2711	4.0143	3.8923	3.8003	3.7708	3.7831
	Nguyen *et al.* (2015)	4.0691	3.7976	3.6636	3.5530	3.4914	3.4830	4.2445	3.9695	3.8387	3.7402	3.7081	3.7214
1-8-1	Present	4.6718	4.1362	3.8504	3.6131	3.4842	3.4526	4.9142	4.3433	4.0478	3.8188	3.7388	3.7410
	Kahya and Turan (2018)	4.7161	4.1749	3.8906	3.6596	3.5432	3.5089	4.9177	4.3464	4.0509	3.8226	3.7438	3.7459

Table 4 Comparision of DFNFs of IP-FG beams without elastic foundations

α	Source	p			
		0.5	1	2	5
0.1	Present	4.5900	4.0675	3.5917	3.3260
	Pandey and Pradyumna (2021)	4.4935	4.0001	3.5647	3.3328
0.2	Present	4.5752	3.9364	3.2769	2.8429
	Pandey and Pradyumna (2021)	4.3664	3.8138	3.2914	2.9906

modes of P-FG beams resting on elastic foundations versus power-law index (p) with those of (Mechab *et al.* 2017, Sayyad and Ghugal 2018). The material properties are taken from the related studies, and $L/h=5$, $k_w=k_p=0$, $\alpha=0$, 0-1-0 SCSTR are considered. As one can see from Table 2 the present findings correspond well with those previously reported.

Study 2: Table 3 presents the comparison of dimensionless fundamental natural frequencies (DFNFs) of P-FGSBs resting on elastic foundations versus p for two different spans to depth ratios (L/h) with those of (Nguyen *et al.* 2015, Nguyen *et al.* 2016, Kahya and Turan 2018). The material properties are taken from the related studies, and $k_w=k_p=0$, $\alpha=0$ are taken into account. As one can see from Table 3 the present results are in good agreement with the results of both of those studies.

Study 3: Table 4 shows the comparison of DFNFs of IP- completely FG beams versus p for two different porosity volume fractions (α) with those of Pandey and Pradyumna (2021). The material properties are taken from the related study as well as $L/h=10$, $k_w=k_p=0$, 0-1-0 SCSTR and H-PDP are employed. As one can see from Table 4 results are in good agreement.

Table 5 Comparison of DFNFs of P-FG beams without elastic foundations

BCs	Source	$L/h=10$	$L/h=30$	$L/h=100$
S–S	Present	2.702	2.738	2.742
	Şimşek (2010)	2.702	2.738	2.742
	Sina *et al*. (2009)	2.695	2.737	2.742
C–F	Present	0.970	0.976	0.977
	Şimşek (2010)	0.970	0.976	0.977
	Sina *et al*. (2009)	0.969	0.976	0.977
C–C	Present	5.885	6.137	6.168
	Şimşek (2010)	5.884	6.177	6.214
	Sina *et al*. (2009)	5.811	6.167	6.212

Study 4: Table 5 presents the comparison of DFNFs of P- completely FG beams versus L/h for three different BCs with those of (Sina *et al.* 2009, Şimşek 2010). The material properties are taken from the associated study as $E_m=70$ GPa; $\rho_m=2700$ kg/m^3; $E_c=380$ GPa; $\rho_c=3800$ kg/m^3; $\nu_m=\nu_c=0.23$, as well as $p=0.3$, $k_w=k_p=0$, $\alpha=0$,0-1-0 SCSTR and H-PDP, as well as DNF that is defined as $\Omega=$

Table 6 The variation of DFNFs of P/IP-FGSBs versus foundation stiffness coefficients

k_w	k_p	Perfect						
		0-1-0	1-2-1	2-2-1	1-1-1	2-1-1	2-1-2	1-8-1
0	0	3.7904	3.6995	3.6670	3.6615	3.6528	3.6432	3.7741
0.1		4.7900	4.6885	4.6921	4.6490	4.6809	4.6272	4.7650
0.2		5.6144	5.5024	5.5304	5.4608	5.5208	5.4359	5.5826
0.3		6.3324	6.2106	6.2574	6.1666	6.2488	6.1389	6.2950
0.1	0.0125	5.7902	5.6758	5.7086	5.6337	5.6993	5.6081	5.7570
0.2		6.4887	6.3648	6.4154	6.3202	6.4070	6.2919	6.4501
0.3		7.1190	6.9861	7.0517	6.9391	7.0440	6.9084	7.0757
0.1	0.025	6.6414	6.5153	6.5696	6.4701	6.5614	6.4413	6.6016
0.2		7.2584	7.1234	7.1923	7.0759	7.1847	7.0447	7.2140
0.3		7.8270	7.6836	7.7651	7.6338	7.7581	7.6003	7.7784
0.1	0.05	8.0790	7.9319	8.0189	7.8810	8.0120	7.8465	8.0285
0.2		8.5934	8.4386	8.5364	8.3855	8.5299	8.3490	8.5392
0.3		9.0787	8.9165	9.0243	8.8613	9.0181	8.8228	9.0210
0.1	0.1	10.3727	10.1904	10.3239	10.1294	10.3184	10.0858	10.3057
0.2		10.7781	10.5896	10.7309	10.5267	10.7254	10.4814	10.7083
0.3		11.1689	10.9742	11.1229	10.9094	11.1176	10.8626	11.0962
k_w	k_p	Imperfect						
		0-1-0	1-2-1	2-2-1	1-1-1	2-1-1	2-1-2	1-8-1
0	0	3.5917	3.6987	3.7104	3.6732	3.6894	3.6545	3.6945
0.1		4.7432	4.7353	4.7660	4.6889	4.7342	4.6540	4.7836
0.2		5.6653	5.5826	5.6269	5.5207	5.5869	5.4740	5.6672
0.3		6.457	6.3172	6.3725	6.2427	6.3256	6.1861	6.4304
0.1	0.0125	5.8599	5.7626	5.8097	5.6977	5.7680	5.6484	5.8545
0.2		6.6284	6.4769	6.5345	6.3997	6.4861	6.3411	6.5961
0.3		7.3166	7.1198	7.1866	7.0320	7.1323	6.9651	7.2623
0.1	0.025	6.7955	6.6327	6.6926	6.5529	6.6428	6.4923	6.7577
0.2		7.4683	7.2619	7.3306	7.1717	7.2751	7.1031	7.4094
0.3		8.0853	7.8407	7.9173	7.7412	7.8566	7.6653	8.0083
0.1	0.05	8.3581	8.0970	8.1771	7.9934	8.1142	7.9145	8.2733
0.2		8.9137	8.6199	8.7070	8.5081	8.6394	8.4227	8.8136
0.3		9.4367	9.1129	9.2064	8.9933	9.1345	8.9020	9.3227
0.1	0.1	10.8264	10.4258	10.5362	10.2860	10.4528	10.1791	10.6774
0.2		11.2609	10.8369	10.9525	10.6908	10.8656	10.5791	11.1013
0.3		11.6792	11.2329	11.3535	11.0808	11.2631	10.9645	11.5096

$\omega L^2/h\sqrt{I_0/A_{11}}$. Table 5 shows that the findings of the present study are in good agreement with the previously published ones.

Study 5: Table 6 demonstrates the variation of DFNFs of P/IP-FGSBs with several SCSTR resting on elastic foundation versus different dimensionless foundation stiffness coefficients, k_w and k_p for $L/h = 10$, $p = 2$, $\alpha = 0.1$, and H-PDP. It is seen that the DFNFs increase with the raise of k_w and k_p for both P/ IP-FGSBs. However, the influence of k_w and k_p becomes more pronounced for IP-FGSBs, as well as the influences of k_w and k_p vary depending on the SCSTR.

Study 6: Table 7 shows the variation of DNFs of IP-FGSBs with/without elastic foundations versus the first three mode numbers (MNs) for $L/h = 10, p = 2, \alpha = 0.1$, $k_w = 0.1$, $k_p = 0.025$, and H-PDP. It is observed that DNFs increase with the increase of the number of modes. The influence of the variation of mode numbers on DNFs of FGSBs becomes less pronounced, the consideration of the WPEFs, especially in the fundamental mode.

Study 7: Table 8 describes the variation of DFNFs of P/IP-FGSBs with/without elastic foundations versus porosity volume fraction (α) for $L/h = 10, p = 2, k_w = 0.1, k_p = 0.025$, and H-PDP. It is found that the DFNFs of FGSBs change according to the SCSTR with the rise of α, irregularly for the foundationless case and Winkler-Pasternak foundations. The increase of α grows the influence of porosity, while the related influence is more obvious in completely FG beams in comparison with FGSBs.

Study 8: Table 9 presents the variation of DFNFs of IP-FGSBs with/without elastic foundations versus power-law index (p) for $L/h = 10, \alpha = 0.1, k_w = 0.1, k_p = 0.025$ and H-PDP. It is seen that DFNFs decrease with the increase of p. The influence of the variation of p on DFNFs of FGSBs changes according to the SCSTR. Besides, the influence of the variation of p on DFNFs of FGSBs loses its efficiency with the consideration of the WPEFs.

Study 9: Table 10 reports the variation of DFNFs of IP-FGSBs with/without elastic foundations versus span to depth ratio (L/h) for $p = 2, \alpha = 0.1, k_w = 0.1, k_p = 0.025$,

Table 7 The variation of DNFs of P/IP-FGSBs with or without elastic foundations versus the first three MNs

SCSTR	Foundationless Case			Winkler-Pasternak Foundations		
	Mode Number			Mode Number		
	1	2	3	1	2	3
0-1-0	3.5918	13.7669	29.1291	6.7955	17.0682	32.5481
2-1-2	3.6545	14.0802	29.9947	6.4923	16.9197	32.8880
2-1-1	3.6894	14.0321	29.4074	6.6428	17.0334	32.5277
1-1-1	3.6732	14.1209	29.9953	6.5529	17.0114	32.9507
2-2-1	3.7104	14.1101	29.5665	6.6926	17.1428	32.7202
1-2-1	3.6987	14.1828	30.0291	6.6327	17.1395	33.0645
1-8-1	3.6945	14.1407	29.8691	6.7577	17.2569	33.0859

Table 8 The variation of DFNFs of P/IP-FGSBs with or without elastic foundations versus porosity volume fraction

SCSTR	Foundationless Case				Winkler-Pasternak Foundations			
	α				α			
	0	0.1	0.15	0.20	0	0.1	0.15	0.20
0-1-0	3.7904	3.5918	3.4542	3.2769	6.6414	6.7955	6.8784	6.9644
2-1-2	3.6432	3.6545	3.6600	3.6653	6.4413	6.4923	6.5182	6.5444
2-1-1	3.6528	3.6894	3.7080	3.7269	6.5614	6.6428	6.6846	6.7272
1-1-1	3.6615	3.6732	3.6782	3.6825	6.4701	6.5529	6.5954	6.6387
2-2-1	3.6670	3.7104	3.7325	3.7548	6.5696	6.6926	6.7568	6.8230
1-2-1	3.6995	3.6987	3.6953	3.6895	6.5153	6.6327	6.6938	6.7566
1-8-1	3.7741	3.6945	3.6398	3.5712	6.6016	6.7577	6.8407	6.9271

Table 9 The variation of DFNFs of IP-FGSBs with or without elastic foundations versus power-law index

SCSTR	Foundationless Case					Winkler-Pasternak Foundations				
	p					*p*				
	0	0.5	1	2	5	0	0.5	1	2	5
0-1-0	5.4662	4.5901	4.0676	3.5918	3.3260	7.4506	7.0743	6.8942	6.7955	6.8570
2-1-2	3.8019	3.7239	3.6866	3.6545	3.6328	6.4693	6.4766	6.4825	6.4923	6.5086
2-1-1	3.6852	3.6801	3.6819	3.6894	3.7044	6.4928	6.5617	6.6001	6.6428	6.6909
1-1-1	3.9753	3.8146	3.7369	3.6732	3.6382	6.5494	6.5402	6.5412	6.5529	6.5832
2-2-1	3.8351	3.7535	3.7233	3.7104	3.7216	6.5307	6.5948	6.6372	6.6926	6.7647
1-2-1	4.2631	3.9671	3.8187	3.6987	3.6430	6.7000	6.6441	6.6266	6.6327	6.6811
1-8-1	4.9374	4.3223	3.9823	3.6945	3.5620	7.1019	6.8867	6.7937	6.7577	6.8294

Table 10 The variation of DFNFs of IP-FGSBs with or without elastic foundations versus span to depth ratio

SCSTR	Foundationless Case					Winkler-Pasternak Foundations				
	L/h					*L/h*				
	5	10	20	50	100	5	10	20	50	100
0-1-0	3.4417	3.5918	3.6334	3.6454	3.6472	4.4680	6.7955	12.1356	29.2060	58.0786
2-1-2	3.5201	3.6545	3.6915	3.7021	3.7036	4.4057	6.4923	11.3857	27.2078	54.0446
2-1-1	3.5080	3.6894	3.7407	3.7555	3.7577	4.4431	6.6428	11.7051	28.0129	55.6563
1-1-1	3.5302	3.6732	3.7127	3.7241	3.7257	4.4316	6.5529	11.5086	27.5156	54.6604
2-2-1	3.5275	3.7104	3.7621	3.7771	3.7793	4.4723	6.6926	11.7993	28.2448	56.1191
1-2-1	3.5457	3.6987	3.7412	3.7534	3.7552	4.4674	6.6327	11.6688	27.9159	55.4608
1-8-1	3.5352	3.6945	3.7389	3.7517	3.7536	4.5056	6.7577	11.9587	28.6757	56.9912

and H-PDP. It is observed that DFNFs decrease with the increase of L/h. The influence of the variation of L/h on DFNFs of FGSBs changes according to the SCSTR. Besides, the influence of the variation of L/h on DFNFs of FGSBs becomes very apparent with the consideration of the WPEFs.

Study 10: Table 11 describes the variation of DFNFs of IP-FGSBs with/without elastic foundations versus distinct PDPs for $L/h = 10, p = 2, \alpha = 0.1, k_w = 0.1, k_p = 0.025$. It is seen that DFNFs change considerably according to the PDPs. The influence of the variation of PDPs on DFNFs of FGSBs varies according to the SCSTR. However, the highest influences of PDPs are observed for H-PDPs while the lowest ones are seen for O-PDPs. Besides, the influence of the variation of PDPs on DFNFs of FGSBs loses its efficiency with the consideration of the WPEFs.

Study 11: Table 12 explains the variation of DFNFs of IP-FGSBs with/without elastic foundations versus different

Table 11 The variation of DFNFs of P/IP-FGSBs with or without elastic foundations versus several PDPs

SCSTR	Perfect	Foundationless Case				Perfect	Winkler-Pasternak Foundations			
		PDP					PDP			
		H	X	O	V		H	X	O	V
0-1-0	3.7904	3.5918	3.6254	3.7868	3.5990	6.6414	6.7955	6.6753	6.6487	6.6605
2-1-2	3.6432	3.6545	3.6484	3.6433	3.6449	6.4413	6.4923	6.4663	6.4417	6.4643
2-1-1	3.6528	3.6894	3.6699	3.6531	3.6681	6.5614	6.6428	6.6011	6.5622	6.6001
1-1-1	3.6615	3.6732	3.6651	3.6617	3.6560	6.4701	6.5529	6.5097	6.4712	6.5046
2-2-1	3.6670	3.7104	3.6840	3.6677	3.6793	6.5696	6.6926	6.6277	6.5715	6.6250
1-2-1	3.6995	3.6987	3.6913	3.6997	3.6734	6.5153	6.6327	6.5684	6.5176	6.5583
1-8-1	3.7741	3.6945	3.7016	3.7731	3.6709	6.6016	6.7577	6.6576	6.6070	6.6404

Table 12 The variation of DFNFs of P/IP-FGSBs with or without elastic foundations versus different BCs

SCSTR	Foundationless Case				Winkler-Pasternak Foundations			
	BCs				BCs			
	C-C	C-F	C-S	S-S	C-C	C-F	C-S	S-S
0-1-0	7.8276	1.2890	5.5452	3.5917	10.0070	6.6488	8.2426	6.7954
2-1-2	8.0089	1.3092	5.6535	3.6545	9.8876	6.2080	8.0087	6.4922
2-1-1	7.9821	1.3268	5.6803	3.6893	9.9682	6.3834	8.1468	6.6427
1-1-1	8.0331	1.3167	5.6780	3.6732	9.9459	6.2760	8.0714	6.5529
2-2-1	8.0269	1.3344	5.7124	3.7103	10.0338	6.4355	8.2039	6.6925
1-2-1	8.0690	1.3268	5.7122	3.6987	10.0255	6.3648	8.1550	6.6327
1-8-1	8.0438	1.3261	5.7016	3.6944	10.10438	6.5332	8.2637	6.7576

BCs for $L/h = 10, p = 2, \alpha = 0.1, k_w = 0.1, k_p = 0.025$ and H-PDP. It is seen that DFNFs change noticeably according to the BCs. The highest DFNFs are observed for C-C BCs while the lowest ones are gotten for C-F BCs. The influence of the BCs on DFNFs of FGSBs stays constant according to the SCSTR. Besides, the influence of the BCs on DFNFs of FGSBs becomes less pronounced with the consideration of the WPEFs.

6. Conclusions

The NFs of P/IP-FGSBs, resting on WPEFs, were investigated in this article. Using TrSDT, the kinematic relation of the P/IP-FGSB resting on the WPEFs was defined, and the equations of motion were derived using Hamilton's principle. Under four separate BCs, a closed-form solution was established for the NF analysis of P/IP-FGSBs resting on WPEFs. The effects of foundation coefficients, mode numbers, porosity volume fraction, power-law index, span to depth ratio, PDPs, SCSTRs, and BCs on the values of the NFs of the P/IP-FGSBs were thoroughly investigated.

To summarize, the following findings were reached:

- DFNFs increase with the raise of foundation stiffness coefficients for FGSBs in all cases
- The influence of the foundation stiffness coefficients on DFNFs becomes more pronounced for IP-FGSBs
- The influence of the power-law index on DFNFs loses its efficiency with the consideration of the WPEFs
- The influence of the span-to-depth ratio on DFNFs becomes very apparent with the consideration of the WPEFs
- The highest influences of PDPs were observed for H-PDPs while the lowest ones were seen for O-PDPs
- The influences of the MNs, PDPs, and BCs on DNFs become less pronounced with the consideration of the WPEFs
- The influences of foundation stiffness coefficients, porosity volume fraction, power-law index, span to depth ratio, and PDPs on NFs vary depending on the SCSTR

Finally, it is determined that the parameters under consideration have a significant impact on the free vibration of FGSBs. Furthermore, the proposed TrSDT not only managed the existing situation properly and yielded good outcomes, but it also eased the current problem. The given solution approach will be expanded in future research for mechanical behaviors of additional sorts of structures built of diverse materials with macro/micro dimensions.

References

Akbaş, Ş.D. (2018), "Forced vibration analysis of functionally graded porous deep beams", *Compos. Struct.*, **186**, 293-302. https://doi.org/10.1016/j.compstruct.2017.12.013U.

Akgöz, B. and Civalek, Ö. (2018), "Vibrational characteristics of embedded microbeams lying on a two-parameter elastic foundation in thermal environment", *Compos. B. Eng.*, **150**, 68-77. https://doi.org/10.1016/j.compositesb.2018.05.049.

Al-Furjan, M.S.H., Farrokhian, A., Keshtegar, B., Kolahchi, R. and Trung, N.T. (2021), "Dynamic stability control of viscoelastic nanocomposite piezoelectric sandwich beams resting on Kerr foundation based on exponential piezoelasticity theory", *Eur. J. Mech. A. Solid.*, **86**, 104169. https://doi.org/10.1016/j.euromechsol.2020.104169.

Al-Furjan, M.S.H., Hatami, A., Habibi, M., Shan, L. and Tounsi, A. (2021), "On the vibrations of the imperfect sandwich higher-order disk with a lactic core using generalize differential quadrature method", *Compos. Struct.*, **257**, 113150. https://doi.org/10.1016/j.compstruct.2020.113150.

Al-Furjan, M.S.H., Xu, M.X., Farrokhian, A., Jafari, G.S., Shen, X. and Kolahchi, R. (2022), "On wave propagation in piezoelectric-auxetic honeycomb-2D-FGM micro-sandwich beams based on modified couple stress and refined zigzag theories", *Wave Random. Complex. Media*, 1-25. https://doi.org/10.1080/17455030.2022.2030499.

Al-Saedi, D.S.J., Masood, S.H., Faizan-Ur-Rab, M., Alomarah, A. and Ponnusamy, P. (2018), "Mechanical properties and energy absorption capability of functionally graded F2BCC lattice fabricated by SLM", *Mater. Des.*, **144**, 32-44. https://doi.org/10.1016/j.matdes.2018.01.059.

Al-Furjan, M.S.H., Yang, Y., Farrokhian, A., Shen, X., Kolahchi, R. and Rajak, D.K. (2021), "Dynamic instability of nanocomposite piezoelectric-leptadenia pyrotechnica rheological elastomer-porous functionally graded materials micro viscoelastic beams at various strain gradient higher-order theories", *Polym. Compos.*, **43**(1), 282-298. https://doi.org/10.1002/pc.26373.

Al Rjoub, Y.S. and Hamad, A.G. (2016), "Free vibration of functionally Euler-Bernoulli and Timoshenko graded porous beams using the transfer matrix method", *KSCE J. Civil Eng.*, **21**(3), 792-806. https://doi.org/10.1007/s12205-016-0149-6.

Alimoradzadeh, M. and Akbas, S.D. (2022), "Nonlinear dynamic behavior of functionally graded beams resting on nonlinear viscoelastic foundation under moving mass in thermal environment", *Struct. Eng. Mech.*, **81**(6), 705-714. https://doi.org/10.12989/sem.2022.81.6.705.

Alnujaie, A., Akbas, S.D., Eltaher, M.A. and Assie, A. (2021), "Forced vibration of a functionally graded porous beam resting on viscoelastic foundation", *Geomech. Eng.*, **24**(1), 91-103. https://doi.org/10.12989/gae.2021.24.1.091.

AlSaid-Alwan, I.H.H.S. and Avcar, M. (2020), "Analytical solution of free vibration of FG beam utilizing different types of beam theories: A comparative study", *Comput. Concrete*, **26**(3), 285-292. https://doi.org/10.12989/cac.2020.26.3.285.

Amirani, M.C., Khalili, S.M.R. and Nemati, N. (2009), "Free vibration analysis of sandwich beam with FG core using the element free Galerkin method", *Compos. Struct.*, **90**(3), 373-379. https://doi.org/10.1016/j.compstruct.2009.03.023.

Asadi-Ghoozhdi, H., Attarnejad, R., Masoodi, A.R. and Majlesi, A. (2022), "Seismic assessment of irregular RC frames with tall ground story incorporating nonlinear soil–structure interaction", *Struct.*, **41**, 159-172. https://doi.org/10.1016/j.istruc.2022.05.001.

Avcar, M. (2019), "Free vibration of imperfect sigmoid and power law functionally graded beams", *Steel Compos. Struct.*, **30**(6), 603-615. https://doi.org/10.12989/scs.2019.30.6.603.

Avcar, M., Hadji, L. and Civalek, O. (2021), "Natural frequency analysis of sigmoid functionally graded sandwich beams in the framework of high order shear deformation theory", *Compos. Struct.*, **276**, 114564. https://doi.org/10.1016/j.compstruct.2021.114564.

Ávila, A.F. (2007), "Failure mode investigation of sandwich beams with functionally graded core", *Compos. Struct.*, **81**(3), 323-330. https://doi.org/10.1016/j.compstruct.2006.08.030.

Babaei, H., Eslami, M.R. and Khorshidvand, A.R. (2020), "Thermal buckling and postbuckling responses of geometrically imperfect FG porous beams based on physical neutral plane", *J. Therm. Stress.*, **43**(1), 109-131. https://doi.org/10.1080/01495739.2019.1660600.

Bao, T. and Liu, Z. (2020), "Evaluation of Winkler model and Pasternak model for dynamic soil-structure interaction analysis of structures partially embedded in soils", *Int. J. Geomech.*, **20**(2), 04019167. https://doi.org/10.1061/(ASCE)GM.1943-5622.0001519.

Bashiri, A.H., Akbas, S.D., Abdelrahman, A.A., Assie, A., Eltaher, M.A. and Mohamed, E.F. (2021), "Vibration of multilayered functionally graded deep beams under thermal load", *Geomech. Eng.*, **24**(6), 545-557. https://doi.org/10.12989/gae.2021.24.6.545.

Bekkaye, T.H.L., Fahsi, B., Bousahla, A.A., Bourada, F., Tounsi, A., Benrahou, K.H., Tounsi, A. and Al-Zahrani, M.M. (2020), "Porosity-dependent mechanical behaviors of FG plate using refined trigonometric shear deformation theory", *Comput. Concrete*, **26**(5), 439-450. https://doi.org/10.12989/cac.2020.26.5.439.

Benahmed, A., Houari, M.S.A., Benyoucef, S., Belakhdar, K. and Tounsi, A. (2017), "A novel quasi-3D hyperbolic shear deformation theory for functionally graded thick rectangular plates on elastic foundation", *Geomech. Eng.*, **12**(1), 9-34. https://doi.org/10.12989/gae.2017.12.1.009.

Bouafia, K., Selim, M.M., Bourada, F., Bousahla, A.A., Bourada, M., Tounsi, A., Bedia, E.A.A. and Tounsi, A. (2021), "Bending and free vibration characteristics of various compositions of FG plates on elastic foundation via quasi 3D HSDT model", *Steel Compos. Struct.*, **41**(4), 487-50.3 https://doi.org/10.12989/scs.2021.41.4.487.

Bouiadjra, R.B., Bachiri, A., Benyoucef, S., Fahsi, B. and Bernard, F. (2020), "An investigation of the thermodynamic effect on the response of FG beam on elastic foundation", *Struct. Eng. Mech.*, **76**(1), 115-127. https://doi.org/10.12989/sem.2020.76.1.115.

Bowles, J.E. (1988), *Foundation Analysis and Design*, McGraw Hill, New York.

Calio, I. and Greco, A. (2013), "Free vibrations of Timoshenko beam-columns on Pasternak foundations", *J. Vib. Control*, **19**(5), 686-696. https://doi.org/10.1177/1077546311433609.

Chaabane, L.A., Bourada, F., Sekkal, M., Zerouati, S., Zaoui, F.Z., Tounsi, A., Derras, A., Bousahla, A.A. and Tounsi, A. (2019), "Analytical study of bending and free vibration responses of functionally graded beams resting on elastic foundation", *Struct. Eng. Mech.*, **71**(2), 185-196. https://doi.org/10.12989/sem.2019.71.2.185.

Chen, D., Yang, J. and Kitipornchai, S. (2019), "Buckling and bending analyses of a novel functionally graded porous plate using Chebyshev-Ritz method", *Arch. Civil Mech. Eng*., **19**(1), 157-170.

Civalek, O. (2013), "Nonlinear dynamic response of laminated plates resting on nonlinear elastic foundations by the discrete singular convolution-differential quadrature coupled approaches", *Compos. B Eng.*, **50**, 171-179. https://doi.org/10.1016/j.compositesb.2013.01.027.

Civalek, O. and Acar, M.H. (2007), "Discrete singular convolution method for the analysis of Mindlin plates on elastic foundations", *Int. J. Press. Vessel. Pip.*, **84**(9), 527-535. https://doi.org/10.1016/j.ijpvp.2007.07.001.

Daikh, A.A., Guerroudj, M., El Adjrami, M. and Megueni, A. (2019), "Thermal buckling of functionally graded sandwich beams", *Adv. Mat. Res.*, **1156**, 43-59. https://doi.org/10.4028/www.scientific.net/AMR.1156.43.

Das, B.M. and Sivakugan, N. (2018), *Principles of Foundation Engineering*, Cengage learning

Delale, F. and Erdogan, F. (1983), "The crack problem for a nonhomogeneous plane", *J. Appl. Mech.*, **50**(3), 609-614. https://doi.org/10.1115/1.3167098.

Djedid, I.K., Benachour, A., Houari, M.S.A., Tounsi, A. and Ameur, M. (2014), "A n-order four variable refined theory for bending and free vibration of functionally graded plates", *Steel Compos. Struct.*, **17**(1), 21-46. https://doi.org/10.12989/scs.2014.17.1.021.

Du, M.J., Liu, J., Ye, W.B., Yang, F. and Lin, G. (2022), "A new semi-analytical approach for bending, buckling and free vibration analyses of power law functionally graded beams", *Struct. Eng. Mech.*, **81**(2), 179-194. https://doi.org/10.12989/sem.2022.81.2.179.

Dutta, S.C. and Roy, R. (2002), "A critical review on idealization and modeling for interaction among soil-foundation-structure

system", *Comput. Struct.*, **80**(20-21), 1579-1594. https://doi.org/10.1016/S0045-7949(02)00115-3.

El-Hassar, S.M., Benyoucef, S., Heireche, H. and Tounsi, A. (2016), "Thermal stability analysis of solar functionally graded plates on elastic foundation using an efficient hyperbolic shear deformation theory", *Geomech. Eng.*, **10**(3), 357-386. https://doi.org/10.12989/gae.2016.10.3.357.

Elmeichea, N., Abbadb, H., Mechabc, I. and Bernard, F. (2020), "Free vibration analysis of functionally graded beams with variable cross-section by the differential quadrature method based on the nonlocal theory", *Struct. Eng. Mech.*, **75**(6), 737-746. https://doi.org/10.12989/sem.2020.75.6.737.

Farrokh, M. and Taharpur, M. (2021), "Optimization of porosity distribution of FGP beams considering buckling strength", *Struct. Eng. Mech.*, **79**(6), 711-722. https://doi.org/10.12989/sem.2021.79.6.711.

Fouda, N., El-Midany, T. and Sadoun, A.M. (2017), "Bending, buckling and vibration of a functionally graded porous beam using finite elements", *J. Appl. Comput. Mech.*, **3**(4), 274-282. https://doi.org/10.22055/Jacm.2017.21924.1121.

Galeban, M.R., Mojahedin, A., Taghavi, Y. and Jabbari, M. (2016), "Free vibration of functionally graded thin beams made of saturated porous materials", *Steel Compos. Struct.*, **21**(5), 999-1016. https://doi.org/10.12989/scs.2016.21.5.999.

Guellil, M., Saidi, H., Bourada, F., Bousahla, A.A., Tounsi, A., Al-Zahrani, M.M., Hussain, M. and Mahmoud, S.R. (2021), "Influences of porosity distributions and boundary conditions on mechanical bending response of functionally graded plates resting on Pasternak foundation", *Steel Compos. Struct.*, **38**(1), 1-15. https://doi.org/10.12989/scs.2021.38.1.001.

Hadji, L. and Avcar, M. (2021), "Free vibration analysis of FG porous sandwich plates under various boundary conditions", *J. Appl. Comput. Mech.*, **7**(2), 505-519. https://doi.org/10.22055/Jacm.2020.35328.2628.

Hadji, L. and Avcar, M. (2021), "Nonlocal free vibration analysis of porous FG nanobeams using hyperbolic shear deformation beam theory", *Adv. Nano. Res.*, **10**(3), 281-293. https://doi.org/10.12989/anr.2021.10.3.281.

Hamed, M.A., Abo-bakr, R.M., Mohamed, S.A. and Eltaher, M.A. (2020), "Influence of axial load function and optimization on static stability of sandwich functionally graded beams with porous core", *Eng. Comput.*, **36**(4), 1929-1946. https://doi.org/10.1007/s00366-020-01023-w.

Han, C., Li, Y., Wang, Q., Wen, S., Wei, Q., Yan, C., Hao, L., Liu, J. and Shi, Y. (2018), "Continuous functionally graded porous titanium scaffolds manufactured by selective laser melting for bone implants", *J Mech Behav Biomed Mater*. **80**, 119-127. https://doi.org/10.1016/j.jmbbm.2018.01.013.

He, S.Y., Zhang, Y., Dai, G. and Jiang, J.Q. (2014), "Preparation of density-graded aluminum foam", *Mater. Sci. Eng.: A*, **618**, 496-499. https://doi.org/10.1016/j.msea.2014.08.087.

Hebali, H., Chikh, A., Bousahla, A.A., Bourada, F., Tounsi, A., Benrahou, K.H., Hussain, M. and Tounsi, A. (2022), "Effect of the variable visco-Pasternak foundations on the bending and dynamic behaviors of FG plates using integral HSDT model", *Geomech. Eng.*, **28**(1), 49-64. https://doi.org/10.12989/gae.2022.28.1.049.

Hetényi, M. (1946), *Beams on Elastic Foundation; Theory with Applications in the Fields of Civil and Mechanical Engineering*, University of Michigan Press, Ann Arbor.

Hong, C.Q., Du, J.C., Liang, J., Zhang, X.H. and Han, J.C. (2011), "Functionally graded porous ceramics with dense surface layer produced by freeze-casting", *Ceram. Int.*, **37**(8), 3717-3722. https://doi.org/10.1016/j.ceramint.2011.04.119.

Jia, J. and Jia (2018), *Soil Dynamics and Foundation Modeling*, Springer.

Kahya, V. and Turan, M. (2018), "Vibration and stability analysis of functionally graded sandwich beams by a multi-layer finite element", *Compos. B Eng.*, **146**, 198-212. https://doi.org/10.1016/j.compositesb.2018.04.011.

Kerr, A.D. (1964), "Elastic and viscoelastic foundation models", *J. Appl. Mech.*, **31**(3), 491-498. https://doi.org/10.1115/1.3629667.

Kieback, B., Neubrand, A. and Riedel, H. (2003), "Processing techniques for functionally graded materials", *Mater. Sci. Eng.: A*, **362**(1-2), 81-105. https://doi.org/10.1016/S0921-5093(03)00578-1.

Kilicer, S., Ozgan, K. and Daloglu, A. (2018), "Effects of soil structure interaction on behavior of reinforced concrete structures", *J. Struct. Eng. Appl. Mech.*, **1**(1), 28-33. https://doi.org/10.31462/jseam.2018.01028033.

Kitipornchai, S., Chen, D. and Yang, J. (2017), "Free vibration and elastic buckling of functionally graded porous beams reinforced by graphene platelets", *Mater. Des.*, **116**, 656-665. https://doi.org/10.1016/j.matdes.2016.12.061.

Koizumi, M. (1997), "FGM activities in Japan", *Compos. B Eng.*, **28**(1-2), 1-4. https://doi.org/10.1016/S1359-8368(96)00016-9.

Kolahchi, R., Bidgoli, A.M.M. and Heydari, M.M. (2015), "Size-dependent bending analysis of FGM nano-sinusoidal plates resting on orthotropic elastic medium", *Struct. Eng. Mech.*, **55**(5), 1001-1014. https://doi.org/10.12989/sem.2015.55.5.1001.

Kolahchi, R., Keshtegar, B. and Trung, N.T. (2021), "Optimization of dynamic properties for laminated multiphase nanocomposite sandwich conical shell in thermal and magnetic conditions", *J Sandw Struct Mater.*, **24**(1), 643-662. https://doi.org/10.1177/10996362211020388.

Liu, G., Wu, S., Shahsavari, D., Karami, B. and Tounsi, A. (2022), "Dynamics of imperfect inhomogeneous nanoplate with exponentially-varying properties resting on viscoelastic foundation", *Eur. J. Mech. A. Solid.*, **95**, 104649. https://doi.org/10.1016/j.euromechsol.2022.104649.

Madenci, E. (2021), "Free vibration and static analyses of metal-ceramic FG beams via high-order variational MFEM", *Steel Compos. Struct.*, **39**(5), 493-509. https://doi.org/10.12989/scs.2021.39.5.493.

Madenci, E. and Ozkilic, Y.O. (2021), "Free vibration analysis of open-cell FG porous beams: analytical, numerical and ANN approaches", *Steel Compos. Struct.*, **40**(2), 157-173. https://doi.org/10.12989/scs.2021.40.2.157.

Matsunaga, H. (1999), "Vibration and buckling of deep beam-columns on two-parameter elastic foundations", *J. Sound Vib.*, **228**(2), 359-376. https://doi.org/10.1006/jsvi.1999.2415.

Mechab, I., El Meiche, N. and Bernard, F. (2017), "Analytical study for the development of a new warping function for high order beam theory", *Compos. B Eng.*, **119**, 18-31. https://doi.org/10.1016/j.compositesb.2017.03.006.

Merzoug, M., Bourada, M., Sekkal, M., Abir, A.C., Chahrazed, B., Benyoucef, S. and Benachour, A. (2020), "2D and quasi 3D computational models for thermoelastic bending of FG beams on variable elastic foundation: Effect of the micromechanical models", *Geomech. Eng.*, **22**(4), 361-374. https://doi.org/10.12989/gae.2020.22.4.361.

Moniri Bidgoli, A.M., Daneshmehr, A.R. and Kolahchi, R. (2014), "Analytical bending solution of fully clamped orthotropic rectangular plates resting on elastic foundations by the finite integral transform method", *J. Appl. Comput. Mech.*, **1**(2), 52-58.

Mu, L. and Zhao, G.P. (2016), "Fundamental frequency analysis of sandwich beams with functionally graded face and metallic foam core", *Shock Vib.*, **2016**, Article ID 3287645. https://doi.org/10.1155/2016/3287645.

Naebe, M. and Shirvanimoghaddam, K. (2016), "Functionally graded materials: A review of fabrication and properties", *Appl. Mater. Today*, **5**, 223-245. https://doi.org/10.1016/j.apmt.2016.10.001.

Nguyen, T.K. and Nguyen, B.D. (2015), "A new higher-order shear deformation theory for static, buckling and free vibration analysis of functionally graded sandwich beams", *J. Sandw. Struct. Mater.*, **17**(6), 613-631. https://doi.org/10.1177/1099636215589237.

Nguyen, T.K., Nguyen, T.T.P., Vo, T.P. and Thai, H.T. (2015), "Vibration and buckling analysis of functionally graded sandwich beams by a new higher-order shear deformation theory", *Compos. B Eng.*, **76**, 273-285. https://doi.org/10.1016/j.compositesb.2015.02.032.

Nguyen, T.K., Vo, T.P., Nguyen, B.D. and Lee, J. (2016), "An analytical solution for buckling and vibration analysis of functionally graded sandwich beams using a quasi-3D shear deformation theory", *Compos. Struct.*, **156**, 238-252. https://doi.org/10.1016/j.compstruct.2015.11.074.

Pandey, S. and Pradyumna, S. (2021), "Thermal shock response of porous functionally graded sandwich curved beam using a new layerwise theory", *Mech. Bas. Des. Struct. Mach.*, 1-26. https://doi.org/10.1080/15397734.2021.1888297.

Pasternak, P.L. (1954), *On a New Method of Analysis of an Elastic Foundation by Means of Two Foundation Constants*, Gosudarstvenrwe Izdatelslvo Literaturi po Stroitclstvu i Arkhitekture, Moscow. (in Russian)

Rabhi, M., Benrahou, K.H., Kaci, A., Houari, M.S.A., Bourada, F., Bousahla, A.A., Tounsi, A., Bedia, E.A.A., Mahmoud, S.R. and Tounsi, A. (2020), "A new innovative 3-unknowns HSDT for buckling and free vibration of exponentially graded sandwich plates resting on elastic foundations under various boundary conditions", *Geomech. Eng.*, **22**(2), 119-132. https://doi.org/10.12989/gae.2020.22.2.119.

Ramteke, P.M., Panda, S.K. and Patel, B. (2022), "Nonlinear eigenfrequency characteristics of multi-directional functionally graded porous panels", *Compos. Struct.*, **279**, 114707. https://doi.org/10.1016/j.compstruct.2021.114707.

Ramteke, P.M., Patel, B. and Panda, S.K. (2021), "Nonlinear eigenfrequency prediction of functionally graded porous structure with different grading patterns", *Wave Random. Complex. Media*, 1-19. https://doi.org/10.1080/17455030.2021.2005850.

Ramteke, P.M., Sharma, N., Choudhary, J., Hissaria, P. and Panda, S.K. (2021), "Multidirectional grading influence on static/dynamic deflection and stress responses of porous FG panel structure: a micromechanical approach", *Eng. Comput.*, 1-21. https://doi.org/10.1007/s00366-021-01449-w.

Rao, N.S.V.K. (2010), *Foundation Design: Theory and Practice*, John Wiley & Sons.

Rao, S.S. (2019), *Vibration of Continuous Systems*, John Wiley & Sons.

Reddy, J.N. (2003), *Mechanics of Laminated Composite Plates and Shells Theory and Analysis*, CRC Press.

Rezaiee-Pajand, M. and Masoodi, A.R. (2016), "Exact natural frequencies and buckling load of functionally graded material tapered beam-columns considering semi-rigid connections", *J. Vib. Control*, **24**(9), 1787-1808. https://doi.org/10.1177/1077546316668932.

Rezaiee-Pajand, M. and Masoodi, A.R. (2022), "Hygro-thermo-elastic nonlinear analysis of functionally graded porous composite thin and moderately thick shallow panels", *Mech. Adv. Mater. Struct.*, **29**(4), 594-612. https://doi.org/10.1080/15376494.2020.1780524.

Rezaiee-Pajand, M., Masoodi, A.R. and Mokhtari, M. (2018), "Static analysis of functionally graded non-prismatic sandwich beams", *Adv. Comput. Des.*, **3**(2), 165-190. https://doi.org/10.12989/acd.2018.3.2.165.

Rezaiee-Pajand, M., Mokhtari, M. and Masoodi, A.R. (2018), "Stability and free vibration analysis of tapered sandwich columns with functionally graded core and flexible connections", *CEAS Aeronaut. J.*, **9**(4), 629-648. https://doi.org/10.1007/s13272-018-0311-6.

Rezaiee-Pajand, M., Rajabzadeh-Safaei, N. and Masoodi, A.R. (2020), "An efficient curved beam element for thermo-mechanical nonlinear analysis of functionally graded porous beams", *Struct.*, **28**, 1035-1049. https://doi.org/10.1016/j.istruc.2020.08.038.

Saidi, H., Tounsi, A. and Bousahla, A.A. (2016), "A simple hyperbolic shear deformation theory for vibration analysis of thick functionally graded rectangular plates resting on elastic foundations", *Geomech. Eng.*, **11**(2), 289-307. https://doi.org/10.12989/gae.2016.11.2.289.

Sayyad, A.S. and Ghugal, Y.M. (2018), "An inverse hyperbolic theory for FG beams resting on Winkler-Pasternak elastic foundation", *Aircraft Spacecraft Sci.*, **5**(6), 671-689. https://doi.org/10.12989/aas.2018.5.6.671.

Sayyad, A.S. and Ghugal, Y.M. (2019), "A sinusoidal beam theory for functionally graded sandwich curved beams", *Compos. Struct.*, **226**, 111246-111246. https://doi.org/10.1016/j.compstruct.2019.111246.

Sayyad, A.S. and Ghugal, Y.M. (2021), "A unified five-degree-of-freedom theory for the bending analysis of softcore and hardcore functionally graded sandwich beams and plates", *J. Sandw. Struct. Mater.*, **23**(2), 473-506. https://doi.org/10.1177/1099636219840980.

Selvadurai, A.P.S. (1979), *Elastic Analysis of Soil-Foundation Interaction*, Elsevier.

Shen, H.S. (2009), *Functionally Graded Materials: Nonlinear Analysis of Plates and Shells*, CRC Press.

Shen, H.S. (2011), "A novel technique for nonlinear analysis of beams on two-parameter elastic foundations", *Int. J. Struct. Stab. Dyn.*, **11**(6), 999-1014. https://doi.org/10.1142/S0219455411004440.

Şimşek, M. (2010), "Fundamental frequency analysis of functionally graded beams by using different higher-order beam theories", *Nucl. Eng. Des.*, **240**(4), 697-705. https://doi.org/10.1016/j.nucengdes.2009.12.013.

Şimşek, M. and Al-shujairi, M. (2017), "Static, free and forced vibration of functionally graded (FG) sandwich beams excited by two successive moving harmonic loads", *Compos. B. Eng.*, **108**, 18-34. https://doi.org/10.1016/j.compositesb.2016.09.098.

Sina, S.A., Navazi, H.M. and Haddadpour, H. (2009), "An analytical method for free vibration analysis of functionally graded beams", *Mater. Des.*, **30**(3), 741-747. https://doi.org/10.1016/j.matdes.2008.05.015.

Songsuwan, W., Pimsarn, M. and Wattanasakulpong, N. (2018), "Dynamic responses of functionally graded sandwich beams resting on elastic foundation under harmonic moving loads", *Int. J. Struct. Stab. Dyn.*, **18**(09), 1850112. https://doi.org/10.1142/S0219455418501122.

Tahir, S.I., Chikh, A., Tounsi, A., Al-Osta, M.A., Al-Dulaijan, S.U. and Al-Zahrani, M.M. (2021), "Wave propagation analysis of a ceramic-metal functionally graded sandwich plate with different porosity distributions in a hygro-thermal environment", *Compos. Struct.*, **269**, 114030. https://doi.org/10.1016/j.compstruct.2021.114030.

Tahir, S.I., Tounsi, A., Chikh, A., Al-Osta, M.A., Al-Dulaijan, S.U. and Al-Zahrani, M.M. (2022), "The effect of three-variable viscoelastic foundation on the wave propagation in functionally graded sandwich plates via a simple quasi-3D HSDT", *Steel Compos. Struct.*, **42**(4), 501-511. https://doi.org/10.12989/scs.2022.42.4.501.

Thieme, M., Wieters, K.P., Bergner, F., Scharnweber, D., Worch, H., Ndop, J., Kim, T.J. and Grill, W. (2001), "Titanium powder sintering for preparation of a porous functionally graded material destined for orthopaedic implants", *J. Mater. Sci. Mater. Med.*, **12**(3), 225-231.

https://doi.org/10.1023/a:1008958914818.
Tossapanon, P. and Wattanasakulpong, N. (2016), "Stability and free vibration of functionally graded sandwich beams resting on two-parameter elastic foundation", *Compos. Struct.*, **142**, 215-225. https://doi.org/10.1016/j.compstruct.2016.01.085.
Trinh, L.C., Vo, T.P., Osofero, A.I. and Lee, J. (2016), "Fundamental frequency analysis of functionally graded sandwich beams based on the state space approach", *Compos. Struct.*, **156**, 263-275. https://doi.org/10.1016/j.compstruct.2015.11.010.
Van Vinh, P. and Tounsi, A. (2021), "The role of spatial variation of the nonlocal parameter on the free vibration of functionally graded sandwich nanoplates", *Eng. Comput.*, 1-19. https://doi.org/10.1007/s00366-021-01475-8.
Venkataraman, S. and Sankar, B.V. (2003), "Elasticity solution for stresses in a sandwich beam with functionally graded core", *AIAA J.*, **41**(12), 2501-2505. https://doi.org/10.2514/2.685341T.
Vo, T.P., Thai, H.T., Nguyen, T.K., Inam, F. and Lee, J. (2015), "Static behaviour of functionally graded sandwich beams using a quasi-3D theory", *Compos. B Eng.*, **68**, 59-74. https://doi.org/10.1016/j.compositesb.2014.08.030.
Vo, T.P., Thai, H.T., Nguyen, T.K., Inam, F. and Lee, J.H. (2015), "A quasi-3D theory for vibration and buckling of functionally graded sandwich beams", *Compos. Struct.*, **119**, 1-12. https://doi.org/10.1016/j.compstruct.2014.08.006.
Vo, T.P., Thai, H.T., Nguyen, T.K., Maheri, A. and Lee, J. (2014), "Finite element model for vibration and buckling of functionally graded sandwich beams based on a refined shear deformation theory", *Eng. Struct.*, **64**, 12-22. https://doi.org/10.1016/j.engstruct.2014.01.029.
Wattanasakulpong, N. and Ungbhakorn, V. (2014), "Linear and nonlinear vibration analysis of elastically restrained ends FGM beams with porosities", *Aerosp. Sci. Technol.*, **32**(1), 111-120. https://doi.org/10.1016/j.ast.2013.12.002.
Wattanasakulpong, N., Chaikittiratana, A. and Pornpeerakeat, S. (2018), "Chebyshev collocation approach for vibration analysis of functionally graded porous beams based on third-order shear deformation theory", *Acta Mech. Sin.*, **34**(6), 1124-1135. https://doi.org/10.1007/s10409-018-0770-3.
Winkler, E. (1867), *Die Lehre von der Elasticitaet und Festigkeit*, Dominicus, Prag.
Wu, H.L., Yang, J. and Kitipornchai, S. (2020), "Mechanical analysis of functionally graded porous structures: A review", *Int. J. Struct. Stab. Dyn.*, **20**(13), 2041015. https://doi.org/10.1142/S0219455420410151.
Xiao, H., Yan, K.M. and She, G.L. (2021), "Study on the characteristics of wave propagation in functionally graded porous square plates", *Geomech. Eng.*, **26**(6), 607-615. https://doi.org/10.12989/gae.2021.26.6.607.
Yahiaoui, M., Tounsi, A., Fahsi, B., Bouiadjra, R.B. and Benyoucef, S. (2018), "The role of micromechanical models in the mechanical response of elastic foundation FG sandwich thick beams", *Struct. Eng. Mech.*, **68**(1), 53-66. https://doi.org/10.12989/sem.2018.68.1.053.
Yokoyama, T. (1996), "Vibration analysis of Timoshenko beam-columns on two-parameter elastic foundations", *Comput. Struct.*, **61**(6), 995-1007. https://doi.org/10.1016/0045-7949(96)00107-1.
Zaitoun, M.W., Chikh, A., Tounsi, A., Sharif, A., Al-Osta, M.A., Al-Dulaijan, S.U. and Al-Zahrani, M.M. (2021), "An efficient computational model for vibration behavior of a functionally graded sandwich plate in a hygrothermal environment with viscoelastic foundation effects", *Eng. Comput.*, 1-15. https://doi.org/10.1007/s00366-021-01498-1.
Zhou, C.C., Wang, P. and Li, W. (2011), "Fabrication of functionally graded porous polymer via supercritical CO_2 foaming", *Compos. B Eng.*, **42**(2), 318-325. https://doi.org/10.1016/j.compositesb.2010.11.001.
Zouatnia, N., Hadji, L. and Kassoul, A. (2018), "An efficient and simple refined theory for free vibration of functionally graded plates under various boundary conditions", *Geomech. Eng.*, **16**(1), 1-9. https://doi.org/10.12989/gae.2018.16.1.001.

CC